Mechanical
Sciences

Open Access

Module-based structure design of wheeled mobile robot

Zirong Luo[1]**, Jianzhong Shang**[1]**, Guowu Wei**[2]**, and Lei Ren**[3]

[1]School of Mechatronics Engineering and Automation,
National University of Defence Technology, Changsha 410073, China
[2]School of Computing, Science and Engineering, University of Salford, Salford M5 4WT, UK
[3]School of Mechanical, Aerospace and Civil Engineering, University of Manchester, Manchester M13 9PL, UK

Correspondence: Zirong Luo (luozirong@nudt.edu.cn), Guowu Wei (g.wei@salford.ac.uk),
and Lei Ren (lei.ren@manchester.ac.uk)

Abstract. This paper proposes an innovative and systematic approach for synthesizing mechanical structures of wheeled mobile robots. The principle and terminologies used for the proposed synthesis method are presented by adopting the concept of modular design, isomorphic and non-isomorphic, and set theory with its associated combinatorial mathematics. The modular-based innovative synthesis and design of wheeled robots were conducted at two levels. Firstly at the module level, by creative design and analysing the structures of classic wheeled robots, a wheel module set containing four types of wheel mechanisms, a suspension module set consisting of five types of suspension frames and a chassis module set composed of five types of rigid or articulated chassis were designed and generalized. Secondly at the synthesis level, two kinds of structure synthesis modes, namely the isomorphic-combination mode and the non-isomorphic combination mode were proposed to synthesize mechanical structures of wheeled robots; which led to 241 structures for wheeled mobile robots including 236 novel ones. Further, mathematical models and a software platform were developed to provide appropriate and intuitive tools for simulating and evaluating performance of the wheeled robots that were proposed in this paper. Eventually, physical prototypes of sample wheeled robots/rovers were developed and tested so as to prove and validate the principle and methodology presented in this paper.

1 Introduction

There is growing interest in space exploration and different kinds of mobile robots have been sent to the Lunar and Martian surfaces for detecting and revealing the mystery of vast space, especially in the solar system that surrounds our planet as indicated by Wilson (2005) and Putz (1998). In most of the space exploration programmes, a proper rover with excellent mobility is required so as to traverse terrains with obstacles such as boulders, desert and small craters, Siegwart et al. (2002). These rovers also need to be able to adapt themselves for harsh environment, including lower gravity, high vacuum, heavy radiation, extremely hot and cold temperature, and weak magnetic field. All these factors make locomotion system a key technology for the development of space exploration wheeled robots/rovers.

The investigation and development of locomotion systems for space exploration rovers such as lunar/moon rovers can be traced back to the Lunokhod 1 for the Lunokhod programme and the Lunar Roving Vehicle (LRV) for the Apollo programme as reported in Putz (1998). After that, quite a number of different rovers were designed and developed mainly through space exploration programmes/projects. These include the rovers developed in the last century such as the Lunokhod 2 lunar rover by Carrier (1992) – a revised version of Lunokhod 1 for the Lunokhod programme; the Marsokhod Mars rover for the Mars-96 expedition programme by Kemurdjian et al. (1992); the Dante legged rover for exploring the Mt. Spurr volcano and the Lunar Rover demonstration project by Krotkov et al. (1994), Bares and Wettergreen (1998) and Kennedy et al. (2001); the NASA "Sojourner" as a six-wheeled rover carried by the "Pathfinder" lander for Mars exploration by Volpe et al. (1997); the "Nomad" (the

rover with a transforming chassis developed at Carnegie Mellon University) by Rollins et al. (1998); and the "Nanokhod" as a micro rover for Mars exploration by Tunstel (1999) and Winnendael and Visentin (1999) developed at the European Space Agency.

Owing to its virtues of small volume, light weight, simplicity, reliable structure as well as technical maturity, wheeled rovers continue to gain popularity in the space exploration research; and various rovers, in form of mobile robots, have been developed in this century. The Field Integrated Design & Operations (FIDO) rover was developed and tested by the JPL for NASA 2003 Mars exploration Rovers(MER) mission, as reported in Tunstel et al. (2002) and Schenker et al. (2003), the latest MER robot is the Curiosity rover launched in 2011, see Arvidson (2016). The "Micro 5", a light-weight rover was designed and constructed with a panted grade assist suspension system aiming for lunar exploration, see Takshi et al. (2003). ESA developed an prototype ExoMars rover to search for evidence of life on Mars, see Michaud et al. (2008); In December 2014, ESA member states approved funding for the rover, to be sent on the second launch in 2018, but insufficient funds had already started to threaten a launch delay until 2020. And more recently, the "Yutu", a lunar rover as called "Jade Rabbit", reported in Ip et al. (2014), was developed and sent to the moon as part of the Chang'e-3 mission.

Expect for the research and development conducted by the government bodies/agencies, space exploration rovers also seized the interest from individual researchers who proposed different rover structures, and simulation and evaluation methods. Using the DARTS/DSHELL framework, Yen and Jain (1999) developed the ROAMS system for rover analysis, modelling and real-time simulation; following this work, Jain et al. (2004) presented ROAMS physics-based simulator for closed-loop simulation and operator-in-the-loop simulation. Fuke and Krotkov (1996) investigated the traverse of a lunar rover on rough terrain by extending and adapting the classic dead reckoning approach. Tao et al. (2006) designed a six-wheeled rover and tested the prototype in an unstructured terrain. Shang et al. (2006a) and Shang et al. (2006b) developed and evaluated a six-wheeled lunar rover prototype based on parallel slider crank suspension. Chen et al. (2009) presented and analysed a lunar rover integrated with a so called obverse and reverse four-linkage suspension. Bartlett et al. (2008) designed and developed a four-wheeled Scarab rover with an adjustable kinematic suspension for mobility and drilling in the lunar cold traps. Wen et al. (2013) identified a four-wheel-rhombus-arranged mobility system as lightweight structure for a novel lunar robotic rover with high mobility and manoeuvrability. Recently, by adopting the concept of reconfigurability, Lionel et al. (2014) proposed the conceptual design of a two-state rover coined "transforming roving-rolling explorer" which is capable of reconfiguring the structure between rolling state and roving state for various tasks; and Aoki et al. (2014) developed two types of deployable three

wheeled rovers, named "Tri-Star IV" aiming for the use of lunar exploration.

Furthermore, in order to evaluate and measure the performance and feasibility of wheeled rovers, theoretical criteria, experimental test platforms and virtual simulation methods have been proposed. Michaud et al. (2006) developed a mars rover chasis evaluation tool labeled RCET to support design, selection and optimisation of space exploration rover. Thueer and Siegwart (2010) presented a theoretical model for the evaluation and comparison of the mobility performance of wheeled, all-terrain robots with respect to terrain-ability by integrating the existing and desired metrics. Ghotbi et al. (2015) put forward a dynamic model for analysing wheeled rovers with particular applications in off-road environments on soft soil by considering the influence of performance caused by the change of design parameters of a rover. Inotsume et al. (2013) constructed the empirical studies for analysing and controlling the rovers to reconfigure themselves to adapt to the target terrain that involves sandy slopes. Ding et al. (2013) established a deformable terrain based experimental platform for analysing and evaluating the rover wheel steering performance and mechanics laying background for optimal design of rover steering mechanisms. In addition, Michaud et al. (2006) developed a rover chassis evaluation tool for the design, selection and optimisation of chassis for space exploration rovers. Yang et al. (2008) developed a rover simulation environment named "RSVE" that uses fractional Brown motion technique and statistical properties for constructing diverse virtual lunar terrain such that the dynamic simulation of the multi-body rover system can be conducted with high reality.

However, according to the literature, very little attention has been devoted to the creative design and synthesis of planetary robot rovers according to Seeni et al. (2010); and most of the performance evaluation models and approaches focus only on one or two of the metrics that are essential for the space exploration wheeled rovers, see Luo et al. (2013). In this paper, it is found that there still remain at least two unsolved issues for the development of wheeled robots/rovers, that is, (a) lack of an efficient innovative design method for synthesizing a large number of novel structures for wheeled robots/rovers; and (b) lack of a comprehensive, efficient and intuitive model and simulation environment for performance evaluation, structure optimization and system selection of wheeled robots/rovers. Therefore, in this paper we attempt to tackle the first issue by presenting an efficient and intuitive structure synthesis approach for generating a substantial amount of structures for n-wheeled rovers; and the second issue by proposing a theoretical model accompanied with a virtual simulation platform for rover performance evaluation and optimization. In our previous research (see Shang et al., 2006a, b; Luo et al., 2013), using creative module design method we have designed and developed several individual of six-wheeled mobile robots. In this paper, a systematic approach is proposed which leads to the synthesis of a large

family of feasible structures that can be used to construct different types of wheeled mobile robots.

The rest of this paper is organized as follows. Section 2 presents the principle of the synthesis method used in this paper with the associated fundamental definitions, terminologies and formulas. Section 3 identifies and characterises three module sets, i.e. the wheel module set, the suspension module set and the chassis module set, that are to be used for the module-base synthesis of rover structures presented in Sect. 4; leading to a large family of four-, six- and eight-wheeled rovers. A mathematical model and a virtual environment platform are then presented, together with development of prototypes of sample rovers and the initial physical test results, in Sect. 5. Subsequently, Sect. 6 delivers a brief conclusions for the results obtained in this paper.

2 Synthesis principle and method

2.1 Module definition and principle

A typical wheeled mobile robot can be regarded as a multibody system formed by three elemental modules, i.e. wheel module, suspension module and chassis (base) module. Each elemental module can be constructed by different mechanisms or rigid/articulated structures. In this paper, the different mechanisms forming different types of wheeled modules, suspension modules and chassis (base) modules are defined in set forms as $W = \{w_1, w_2, \ldots, w_L\}$, $S = \{s_1, s_2, \ldots, s_M\}$, and $B = \{b_1, b_2, \ldots, b_N\}$ respectively, where the subscripts L, M and N are, respectively, the numbers of mechanisms or structures that can be selected to construct the wheel module, suspension module and chassis module.

To construct and design a particular wheeled mobile robot R_i, mono- or multi-type of mechanisms or structures in each of the three module sets can be chosen. As illustrated in Fig. 1, a wheeled robot, denoted as R_i, is the combination of the wheel module subset, the suspension module subset and the chassis module subset represented as

$$R_i = \{\{W_i, S_i, B_i\} \mid W_i \subset W, S_i \subset S \text{ and } B_i \subset B\} \quad (1)$$

where, the configurations W_i, S_i and B_i are subsets of the modular sets W, S and B, respectively.

The term "degree of choice" (DOC) denoted as D_C is defined herein to represent the choices in each individual modular set. For example, if only one type of mechanism in the wheel module set is selected for constructing a specified wheeled robot, we denote $D_C(W_i) = 1$, if two types of mechanisms in the wheel module set are chosen for constructing a wheeled robot, it has $D_C(W_i) = 2$, and if l types of mechanisms in the wheel module set that are chosen, it gives $D_C(W_i) = l$, where W_i is a subset of W denoting the ith combination of the wheel module. Similarly, the degree of choice (DOC) for the suspension module and chassis module can be expressed as $D_C(S_i) = m$ and $D_C(B_i) = n$, with S_i and B_i, standing for the subsets of S and B, respectively,

representing the ith combination of the suspension module and the chassis module.

Based on the above definition, the whole wheeled mobile robot set to be synthesized and designed in this paper can be expressed as

$$R = \{R_1, R_2, \ldots, R_k\} \quad (2)$$

where k denotes the kth combination of wheeled robots that can be synthesized and constructed.

2.2 Module based isomorphic and non-isomorphic combination

From the mechanism point of view, two kinematic chains or mechanisms are said to be isomorphic if they share the same topological structure (Tsai, 2000). In this paper, we extend this concept for the combinations of the wheel module, suspension module and chassis module so as to synthesize and construct various types of structures for wheeled mobile robots.

Definition 1. For a wheeled robot $R_i = \{W_i, S_i, B_i\}$, if all of its three modules, i.e. the wheel module W_i, the suspension module S_i, and the chassis module B_i are configured with solo type of mechanisms/structures, which means the wheeled robot has all the three modules with degree of choice (DOC) of one as $D_C(W_i) = D_C(S_i) = D_C(B_i) = 1$, and if the structure of a wheeled robot is synthesized by a combination satisfying

$$D_C(W_i) = 1 \wedge D_C(S_i) = 1 \wedge D_C(B_i) = 1 \quad (3)$$

the combination mode is defined as an *isomorphic combination*. Where the symbol "∧" stands for logical "and".

Definition 2. For any robot $R_i = \{W_i, S_i, B_i\}$, if at least one of its modules has a degree of choice (DOC) that does not equal one as

$$D_C(W_i) \neq 1 \vee D_C(S_i) \neq 1 \vee D_C(B_i) \neq 1 \quad (4)$$

the combination mode is defined as a *non-isomorphic combination*. In Eq. (4), the symbol "∨" denotes logical "or".

2.3 Structure synthesis of wheeled mobile robot

According to the above definition of isomorphic and non-isomorphic combinations, the modular-based structure design of wheeled robots can be achieved through two kinds of basic synthesis modes, i.e. isomorphic-combination synthesis mode denoted as set R_I and non-isomorphic-combination synthesis mode indicated as set R_{NI}. Thus the whole set of wheeled robots R that can be synthesized and obtained is

$$R = R_I \cup R_{NI} \quad (5)$$

where R_I and R_{NI} respectively denote the sets of wheeled robots synthesized from the isomorphic-combination synthesis mode and the non-isomorphic-combination synthesis mode.
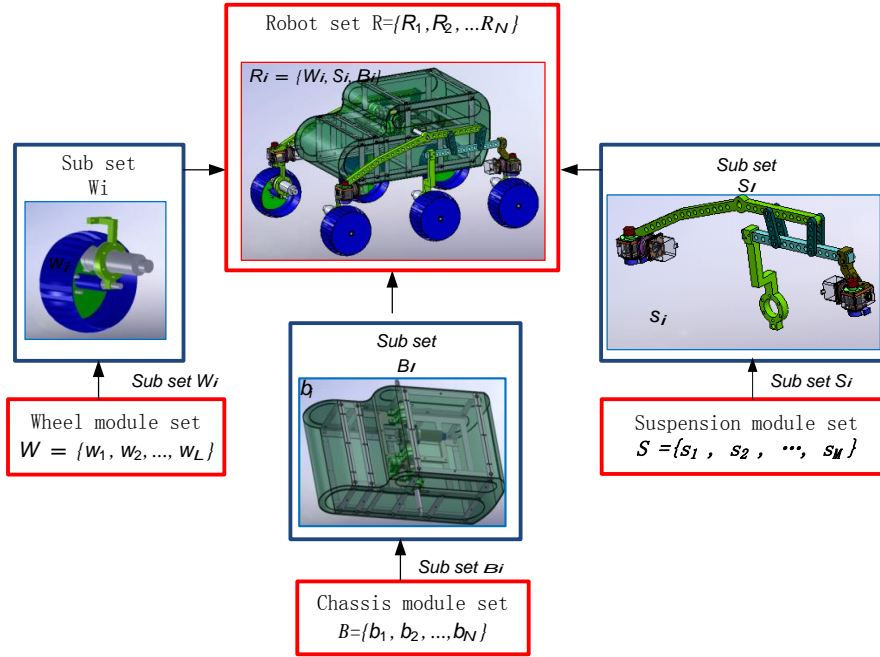
Figure 1. Module sets and Robot set.

2.3.1 Isomorphic-combination synthesis mode

According to the definition of isomorphic combination in Sect. 2.1, any robot R_i synthesized based on the isomorphic-combination mode, which belongs to R_I, can be written as

$$R_i = \{\{W_i, S_i, B_i\} \mid \forall R_i \in R_I\} \tag{6}$$

Where each component module subset, i.e. W_i, S_i and B_i must satisfy the condition presented in Eq. (3), there are three presuppositions provided: (a) the DOC of the wheel module set W is $D_C(W) = L$, (b) the DOC of the suspension module set S is $D_C(S) = M$ and (c) the DOC of the chassis module set B is $D_C(B) = N$.

In this case, according to the above definition, the degrees of choice for each R_i obtained from the isomorphic-combination synthesis mode can be computed as

$$D_C(R_I) = D_C(W) \times D_C(S) \times D_C(B) = L \times M \times N \tag{7}$$

Thus, the total number of wheeled robots $N(R_I)$ that can be obtained by the isomorphic-combination synthesis mode is

$$N(R_I) = L \times M \times N \tag{8}$$

2.3.2 Non-isomorphic-combination synthesis mode

Similarly, we consider the set of wheeled robots R_{NI} that can be obtained with non-isomorphic-combination synthesis mode. In this case, the three presuppositions presented in the

isomorphic-combination synthesis mode still hold such that $D_C(W) = L$, $D_C(S) = M$ and $D_C(B) = N$.

In this synthesis mode, the structure of a wheeled robot R_i is described as

$$R_i = \{\{W_i, S_i, B_i\} \mid \forall R_i \in R_{NI}\} \tag{9}$$

where the three component module subsets W_i, S_i and B_i must comply with the rule indicated in Eq. (4).

In this case, the degrees of choice of structures for a wheeled robot R_i can be calculated as

$$D_C(R_{NI}) = \sum_{l_{\min}}^{l_{\max}} C_L^l \times \sum_{m_{\min}}^{m_{\max}} C_M^m \times \sum_{n_{\min}}^{n_{\max}} C_N^n \tag{10}$$

Where, C_p^k denotes the k-combination of a set with p elements, and l, m and n are, as aforementioned, respectively the numbers of wheel mechanisms/structures that are used to configure the l-combination wheel module subset such that $D_C(W_i) = l$, the m-combination suspension module subset so that $D_C(S_i) = m$ and the n-combination chassis module subset with $D_C(B_i) = n$.

Since in most practical case each structure of a wheeled robot is formed by a suspension module subset of one member as well as a chassis module subset of one member, such that in the most common design case, there exist $m_{\max} = m_{\min} = D_C(S_i) = 1$ and $n_{\max} = n_{\min} = D_C(B_i) = 1$, which implies that in the non-isomorphic-combination synthesis mode there must have $l_{\min} = D_C(W_i) \geq 2$. Substituting these
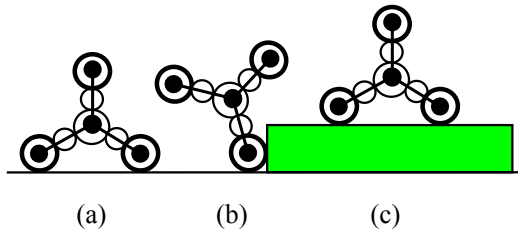
Figure 2. Exterior-planetary wheel.

Figure 3. Planetary-tracked wheel and its working phases.

into Eq. (10), it has

$$D_C(R_{NI}) = \sum_{l=2}^{l_{max}} C_L^l \times C_M^1 \times C_N^1 = \sum_{l=2}^{l_{max}} C_L^l \times M \times N \quad (11)$$

Then, the total number of wheeled robots that can be attained in the non-isomorphic-combination synthesis mode is

$$N(R_{NI}) = \sum_{l=2}^{l_{max}} C_L^l \times M \times N \quad (12)$$

In both Eqs. (11) and (12), there is $l = D_C(W_i) \in [2, L]$, and $L = D_C(W)$, $M = D_C(S)$ and $N = D_C(B)$.

3 Innovative design and characterization of elemental modules

The modular-based innovative synthesis and structure design of wheeled robots can be accomplished at two levels, i.e. elemental level and synthesis level. The elemental module level aims to identify and design the three component modules of a wheeled robot including the wheel module, the suspension module and the chassis module; and the synthesis level aims to get all possible and feasible kinds of design solutions based on the above the isomorphic-combination synthesis mode and the non-isomorphic-combination synthesis mode.

In this section, we focus on the creative design and characterization of the three elemental component modules.

3.1 Innovation and characterization of the wheel module

According to Haggart and Waydo (2008), different kinds of mechanisms/structures have been adapted to design the wheel module for constructing various wheeled robots. In this paper, two classical wheel structures w_1 and w_2 are selected for structure design and synthesis, as listed in Table 1.

The integration wheel, denoted as w_1 which is constructed by enveloped structure, is a simple, compact and reliable design scheme for planetary robot. However, it is hard for this kind of wheel to overwhelm obstacle that is higher than half of its radius. The exterior-planetary wheel w_2, consisting of three evenly distributed wheels driven by a central geared wheel, can conquer high obstacle like stairs. As indicated in
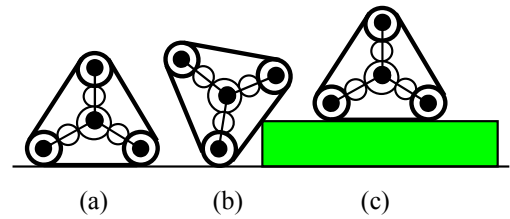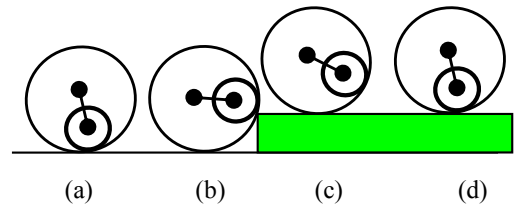

Figure 4. Interior-planetary wheel and its working phases.

Fig. 2, when it encounters an obstacle, the wheel frame turns around and cross the obstacle. This kind of wheel has excellent obstacle-crossing capability and ground adaptability, but due to the multiple contact points between the wheel and the ground, steering of robot with this kind of wheels is inefficient, which mainly relies on the differential motion of the wheels.

By reflecting on the advantages and disadvantages of the integration wheel and the exterior-planetary wheel, this paper proposes two novel wheel modules, i.e. the planetary-tracked wheel w_3 and the interior-planetary wheel w_4 (see Table 1). The planetary-tracked wheel module w_3 has the advantages of both the tracked and exterior planetary wheels. Using this structure, when the obstacle is small, the wheel negotiates obstacle like common tracked robot, as shown in Fig. 3a; in case the wheel encounters a big obstacle as the green block shown in Fig. 3c, it turns around its axle and negotiate the obstacle to cross over, as shown in Fig. 3b.

The interior-planetary wheel w_4 is a novel one constructed based on interior planetary system, as shown in Fig. 4, it has excellent obstacle-crossing capability and flexible steering ability. When the exterior wheel hits on an obstacle (see Fig. 4a and b), the interior geared wheel continues to climb and once the mass centre of the interior wheel is higher than the obstacle, the whole wheel gains the capability to cross the obstacle as illustrated in Fig. 4c and d.

All the four wheel mechanisms/structures listed in Table 1 form a wheel module set $W = \{w_1, w_2, w_3, w_4\}$ to be used in this paper for synthesising structures of wheeled robots.

Table 1. Four types of wheel modules.

Module name	Illustrative diagram	Description
Integration wheel w_1 (classical wheel module)		Integrating driving, steering and sensor in the volume of wheel, this kind of wheel is utilized in the Rocky series robots, Krotkov et al. (1994).
Exterior planetary wheel w_2 (classical wheel module)		Excellent obstacle-crossing capability and ground adaptability. But robot steering can only be realized by differential speeds of wheels.
Planetary tracked wheel w_3 (novel wheel module)		Combining the advantages of tacked and exterior planetary wheel, it has better ground adaptability and obstacle-crossing ability comparing to w_1 and w_2.
Interior planetary wheel w_4 (novel wheel module)		Excellent obstacle-crossing capability and flexible steering ability. However, its motion control is more complex than w_1, w_2, w_3 due to the interior planetary gears.

3.2 Identification and innovation of the suspension module

The typical suspensions used in wheeled robots are active or adaptive. In this paper, in order to synthesize and construct different types of wheeled robots, three classical suspension structures s_1, s_2 and s_3 are selected, and two novel structures are proposed as listed in Table 2.

The two-wheeled rigid suspension s_1 is proved to be a simple, compact and reliable choice for the four-wheeled robot (Krotkov et al., 1994). However, it can only implement undulation equalization once by the rotation of whole suspension, it cannot efficiently improve the motion smoothness and obstacle negotiation. The three-wheeled rocker-boogie suspension s_2 has been proved to be a successful suspension for the Mars exploration rover (Huntsberger et al., 2002; Richard, 2005), compared to suspension s_1, it can implement undulation equalization twice by the rotation of primary and secondary rockers. Similarly, the four-wheeled rocker-boogie suspension s_3 can implement twice undulation equalization by the rotation of primary and secondary rockers. The schemes of these three suspensions are shown in Fig. 5.

In addition, two kinds of new suspension structures are put forward in this paper, one is the parallel slider-crank suspension (Shang et al., 2006a, b) s_4 and the other is a four-bar-linkage-integrated suspension s_5, as listed in Table 2. For the parallel slider-crank suspension, the wheels can overcome obstacle by the slider's linear motion relative to the frame, which can reduce the vertical motion of robot and keep all wheels contact with the surface when it travels on bumpy terrain, as illustrated in Fig. 6.

The four-bar-linkage-integrated suspension s_5 is an innovative variation of the rocker-boogie suspension which re-

(a) Rigid suspension

(b) Rocker-bogie suspension

(c) Four-wheeled rocker-bogie suspension

Figure 5. Three typical suspension modules.
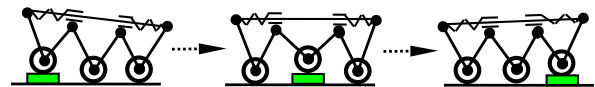
Figure 6. A parallel slider-crank suspension.

places the rockers with a four-bar linkage (see Fig. 7). This design helps to moderate the rotation of the rocker and produces a better mobility due to feature that the instant rotation centre of link 4 is beneath the frame.

Table 2. Five types of suspension structures.

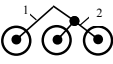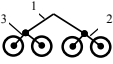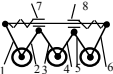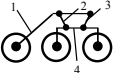| Module name	Illustrative diagram	Description
Rigid suspension s_1 (classical suspension)		Wheels match ground by the rotation of whole suspension 1.
Rocker-boogie suspension s_2 (classical suspension)		Wheels match ground by the rotation between primary rocker 1 and secondary rocker 2.
Four-wheeled rocker-boogie suspension s_3 (classical suspension)		Wheels match ground by the rotations of primary rockers 1 and secondary rockers 2 and 3.
Parallel slider crank suspension s_4 (novel suspension)		Wheels' vertical displacements are transformed smoothly into the horizontal displacements of sliders 7 and 8.
Four-bar-linkage-integrated suspension s_5 (novel suspension)		The instant rotation centre of link 4 is below the ground, which helps robot cross the obstacle.
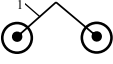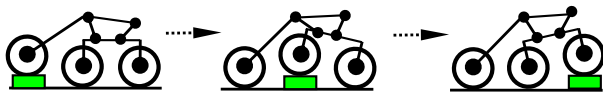
Figure 7. A four-Bar-linkage-integrated suspension.

The above five suspension structures compose a suspension module set $S = \{s_1, s_2, s_3, s_4, s_5\}$, as listed in Table 2, for constructing wheeled robots in Sect. 4.

3.3 Design and identification of the chassis module

Five types of rigid or articulated structures are selected in this paper to form a chassis module set for synthesis and design of wheeled robots, denoted as $B = \{b_1, b_2, b_3, b_4, b_5\}$. They are the rigid-shaft chassis b_1, the elastic-shaft chassis b_2, the differential-geared chassis b_3, the right-and-left segmented chassis b_4 and the fore-and-aft segmented chassis b_5 as listed and illustrated in Table 3.

The elastic shaft chassis b_2, as shown in Table 3, consists of two symmetric elastic shafts 1 and a frame 2. One end of the elastic shaft is connected to the frame end, and the other end is connected to a corresponding suspension such that the two suspensions can rotate independently relative to the frame.

The differential chassis b_3, as shown in the third row of Table 3, consists of a pair of coaxial pinions denoted as 1 and 2, a gear 3 and a frame 4, this mechanism makes it possible for the two suspensions connected to shafts of bevel gears 1 and 2 to rotate in opposite directions without turning the frame. It is interesting to note that, if one of the suspension is held stationary and the other one is free to rotate, the frame can turn at the half speed of the suspension. This characteristic

helps to achieve motion smoothness when the robot crosses an obstacle.

The right-and-left segmented chassis b_4, as shown in the fourth row of Table 3, essentially contains a left segmented chassis 1, a right segmented chassis 2 and a shaft 3. Compared to the differential chassis b_3, the suspensions connected to this kind of chassis turn together with the segmented chassis around shaft 3 which helps the suspensions match the change of terrains.

4 Module-based structure synthesis of reconfigurable wheeled robots

The design theory of vehicles demonstrates that the vehicle mobility and complexity increase with the increase of wheel number; once the number of wheels is determined, the design of suspension and wheel mechanisms/structures follows. According to the state-of-the-art of wheeled robots, researchers mainly adopt 4, 6 and 8 wheels. Hence, considering the practical applications, this paper mainly focuses on synthesis of the 4-, 6- and 8-wheeled robots; the method proposed here can be extended to the synthesis of n-wheeled robots.

4.1 Isomorphic-combination synthesis and construction of wheeled robots

4.1.1 Synthesis of reconfigurable four-wheeled robots

For the synthesis and design of four-wheeled robots based on isomorphic-combination synthesis mode, the component modules identified and proposed in Sect. 3 to be used are: (a) the wheel module set $W = \{w_1, w_2, w_3, w_4\}$, (b) the suspension module subset $S = \{s_1\}$, and (c) the chassis module set $B = \{b_1, b_2, b_3, b_4, b_5\}$ including the integrated chassis modules and segmented chassis modules.

Table 3. Five selected chassis modules.

Module name	Illustrative diagram	Description
Rigid-shaft chassis b_1		Left and right suspensions are fixed with chassis through a rigid shaft 1, this is a rigid chassis.
Elastic-shaft chassis b_2		Left and right suspensions are connected to chassis through an elastic shaft 1, therefore the suspensions can rotate relatively to chassis through the torsion of elastic shaft.
Differential chassis b_3		Left and right suspensions are connected to chassis through a differential gear shaft. Therefore, the chassis's pitch is half of that of the suspensions. It provides a good traverse smoothness.
Right-and-left segmented chassis b_4		Suspensions are fixed to right and left segment chassis 1 and 2 respectively, while the segmented chassis can rotate relatively around shaft 3.
Fore-and-aft segmented chassis b_5		Suspensions and wheels are fixed to fore-and-aft chassis respectively, while the segmented chassis can rotate relatively around shaft 3.

In practical design, for a four-wheeled robot, the suspension and chassis can be reconfigured in the layouts of left-and-right or fore-and-aft mode. Here we consider the left-and-right mode first. According to Eq. (7), the degrees of choice of the four-wheeled robots that can be synthesized with the chassis module set B is

$$D_C(R_{I4-1}) = D_C(W) \times D_C(S) \times D_C(B) = 4 \times 1 \times 5 = 20 \tag{13}$$

As aforementioned, D_C stands for degrees of choice. R_{I4-1} denotes the set of wheeled robot with subscripts I standing for isomorphic-combination synthesis, "4" denoting four wheels and "1" standing for the left-and right mode.

An example structure, i.e. w_2-b_3-s_1 for a four-wheeled robot with suspension of left-and-right layout is illustrated in Fig. 8, the planetary-tracked wheels w_2 and the rigid suspensions s_1 are integrated on both the left and right sides of a differential chassis b_3.

In this layout mode, as listed in Table 4, by adopting integrated chassis modules including b_1, b_2 and b_3, and wheel modules w_1, w_2, w_3 and w_4, 12 design schemes can be obtained. In the table, schemes w_2-b_1-s_1* and w_1-b_1-s_1* are existing schemes, and the rest 10 designs are new ones; while by adopting segmented chassis in which case only b_4 is feasible, 4 more design schemes can be achieved as indicated in the last low of Table 4 and they are all new structures. In the table and hereafter, the scheme with superscript "*" indicates
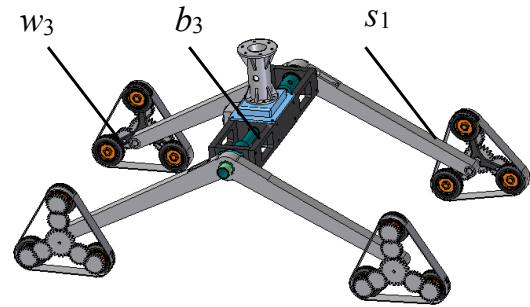
Figure 8. Type w_3-b_3-s_1 structure for a four-wheeled robot in left-and-right layout.

Table 4. Structures of four-wheeled robots in left-and-right layout R_{I4-1}.

	w_1	w_2	w_3	w_4
b_1	w_1-b_1-s_1*	w_2-b_1-s_1*	w_3-b_1-s_1	w_4-b_1-s_1
b_2	w_1-b_2-s_1	w_2-b_2-s_1	w_3-b_2-s_1	w_4-b_2-s_1
b_3	w_1-b_3-s_1	w_2-b_3-s_1	w_3-b_3-s_1	w_4-b_3-s_1
b_4	w_1-b_4-s_1	w_2-b_4-s_1	w_3-b_4-s_1	w_4-b_4-s_1

that it is an existing scheme that can be found in existing literature.

The analysis above indicates that, under the left-and-right layout, by excluding the cases involving chassis module b_5, there are totally of 16 design schemes being synthesized, of
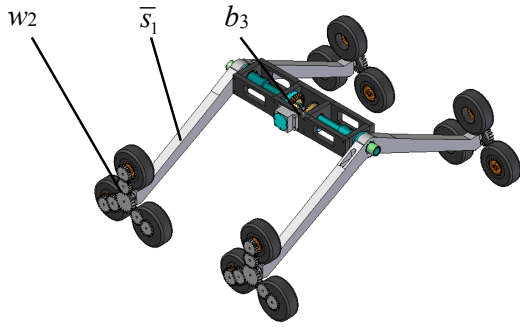
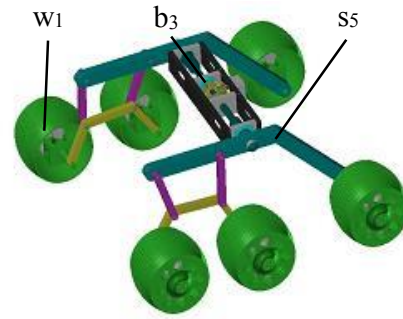**Figure 9.** Type w_2-b_3-$\overline{s}_1$ structure for a four-wheeled robot in fore-and-aft layout.

Table 5. Structures for four-wheeled robots in fore-and-aft layout R_{I4-2}.

	w_1	w_2	w_3	w_4
b_1	w_1-b_1-$\overline{s}_1^+$	w_2-b_1-$\overline{s}_1^+$	w_3-b_1-$\overline{s}_1^+$	w_4-b_1-$\overline{s}_1^+$
b_2	w_1-b_2-$\overline{s}_1$	w_2-b_2-$\overline{s}_1$	w_3-b_2-$\overline{s}_1$	w_4-b_2-$\overline{s}_1$
b_3	w_1-b_3-$\overline{s}_1$	w_2-b_3-$\overline{s}_1$	w_3-b_3-$\overline{s}_1$	w_4-b_3-$\overline{s}_1$
b_4	w_1-b_4-$\overline{s}_1^+$	w_2-b_4-$\overline{s}_1^+$	w_3-b_4-$\overline{s}_1^+$	w_4-b_4-$\overline{s}_1^+$
b_5	w_1-b_5-$\overline{s}_1*$	w_2-b_5-$\overline{s}_1$	w_3-b_5-$\overline{s}_1$	w_4-b_5-$\overline{s}_1$

which only two are existed, and the remaining 14 are new schemes.

Further, by reconfiguring the suspension system, structures of wheeled robots with suspensions in the fore-and-aft layout can be synthesized and one example, i.e. w_2-b_3-$\overline{s}_1$ is illustrated in Fig. 9, which has four exterior-planetary-tracked wheels w_2 and two rigid suspensions $\overline{s}_1$ of fore-and-aft layout assembled in a differential chassis b_3.

In this layout mode, 20 structures denoted as $D_C(R_{I4-2})$ can be synthesized as listed in Table 5. By adopting integrated body modules including b_1, b_2 and b_3, and wheel modules including w_1, w_2, w_3 and w_4, 12 design schemes can be obtained. Considering the 4 design schemes listed in the first row of Table 5 (denoted with superscript "+" in the end) that are composed of the suspension module $\overline{s}_1$, the rigid chassis module b_1 and all of the four wheel modules, they are functionally the same as the four schemes that are listed in the first row of Table 4. Thus 8 types of design schemes are actually attained and they are all new. Subsequently, by adopting the segmented chassis including modules b_4 and b_5, 8 more design schemes can be synthesized in which w_1-b_4-$\overline{s}_1$ and w_1-b_5-$\overline{s}_1$ are existing schemes, considering the four schemes including fore-and aft layout of chassis b_4 (denoted with superscript "+" in the end) is logically same as the four design schemes including chassis b_5, and hence 3 of them are new.

From the above analysis, in isomorphic-combination synthesis mode 28 structures for the four-wheeled robot can be synthesized in which 25 of them are new. Therefore, the de-

grees of choice of structures for four-wheeled robot synthesized based on the isomorphic-combination synthesis mode is

$$D_C(R_{I4}) = D_C(R_{I4-1}) + D_C(R_{I4-2}) - 4 = 16 + 20 - 8 = 28 \tag{14}$$

where, R_{I4} denote the structure of four-wheeled robot obtained in the isomorphic-combination synthesis mode. And thus using Eq. (8), the number of structures of the robots synthesized in this section is $N(R_{I4}) = D_C(R_{I4}) = 28$.

4.1.2 Synthesis of six-wheeled robots

In order to synthesize six-wheeled robots, in isomorphic-combination synthesis mode, component modules considered are: (a) the wheel module subset $W = \{w_1, w_2, w_3, w_4\}$, (b) the suspension module subset $S_2 = \{s_2, s_4, s_5\}$, and (c) the integrated chassis module set $B_3 = \{b_2, b_3, b_4\}$. According to Eq. (7), degrees of choice of six-wheeled robot that can be synthesized is

$$D_C(R_{I6}) = D_C(W) \times D_C(S_2) \times D_C(B_3) = 4 \times 3 \times 3 = 36 \tag{15}$$

The structure of an example six-wheeled robot that is synthesized with the isomorphic-combination synthesis mode by integrating an integration wheel module w_1, a four-bar linkage integrated suspension s_5 and a differential chassis b_3 is illustrated in Fig. 10. This is a type w_1-b_3-s_5 structure in which the four-bar linkage integrated suspension helps realize twice undulations when crossing obstacles.

Referring to Eq. (8), we know that there are $N(R_{I6}) = D_C(R_{I6}) = 36$ design schemes that can be synthesized in this category. These structures are listed in Table 6, in which only 1 design scheme (w_1-b_3-s_2*) can be found in the literature (see Table 13) and the others are all new.

4.1.3 Synthesis of eight-wheeled robots

Similarly, based on the isomorphic-combination synthesis mode, eight-wheeled mobile robot can be constructed. In this

Figure 10. Type w_1-b_3-s_5 structure for a six-wheeled robot.

Table 6. Structures for six-wheeled robots R_{I6}.

	w_1	w_2
b_2	w_1-b_2-s_2, w_1-b_2-s_4, w_1-b_2-s_5	w_2-b_2-s_2, w_2-b_2-s_4, w_2-b_2-s_5
b_3	w_1-b_3-s_2*, w_1-b_3-s_4, w_1-b_3-s_5	w_2-b_3-s_2, w_2-b_3-s_4, w_2-b_3-s_5
b_4	w_1-b_4-s_2, w_1-b_4-s_4, w_1-b_4-s_5	w_2-b_4-s_2, w_2-b_4-s_4, w_2-b_4-s_5

	w_3	w_4
b_2	w_3-b_2-s_2, w_3-b_2-s_4, w_3-b_2-s_5	w_4-b_2-s_2, w_4-b_2-s_4, w_4-b_2-s_5
b_3	w_3-b_3-s_2, w_3-b_3-s_4, w_3-b_3-s_5	w_4-b_3-s_2, w_4-b_3-s_4, w_4-b_3-s_5
b_4	w_3-b_4-s_2, w_3-b_4-s_4, w_3-b_4-s_5	w_4-b_4-s_2, w_4-b_4-s_4, w_4-b_4-s_5

Table 7. Structures for eight-wheeled robots R_{I8}.

	w_1	w_2	w_3	w_4
b_2	w_1-b_2-s_3	w_2-b_2-s_3	w_3-b_2-s_3	w_4-b_2-s_3
b_3	w_1-b_3-s_3*	w_2-b_3-s_3	w_3-b_3-s_3	w_4-b_3-s_3
b_4	w_1-b_4-s_3	w_2-b_4-s_3	w_3-b_4-s_3	w_4-b_4-s_3

Figure 11. Type w_4-b_4-s_3 structure of an eight-wheeled robot.

case, the whole wheel module set $W = \{w_1, w_2, w_3, w_4\}$ and the integrated chassis module subset $B_3 = \{b_2, b_3, b_4\}$ are used for the synthesis. However, only the suspension module subset $S_3 = \{s_3\}$ can be used for this synthesis. Thus, the degrees of choice of the wheel, suspension and chassis modules are $D_C(W) = 4$, $D_C(S_3) = 1$ and $D_C(B_3) = 3$, respectively. Substituting these into Eqs. (7) and (8), the degrees of choice i.e. the number of eight-wheeled robots that can be synthesized is

$$N(R_{I8}) = D_C(R_{I8}) = D_C(W) \times D_C(S_3) \times D_C(B_3)$$
$$= 4 \times 1 \times 3 = 12 \qquad (16)$$

Hence, 12 design schemes can be attained in this synthesis scheme. They are listed in Table 7 and one of the schemes, i.e. w_1-b_3-s_3* can be found in the literature, thus 11 of them are new schemes. An example of the structure, i.e. type w_4-b_4-s_3 for an eight-wheeled rovers that is constructed by combining an interior-planetary wheel module w_4, a four-wheeled rocker-bogie suspension module s_3 and a right-and-left segmented chassis module b_4 is illustrated in Fig. 10.

Hence, based on the isomorphic-combination approach, totally 76 types of structures for wheeled robots are synthesized as

$$N(R_I) = D_C(R_I) = D_C(R_{I4}) + D_C(R_{I6}) + D_C(R_{I8})$$
$$= 28 + 36 + 12 = 76 \qquad (17)$$

In these 76 types, 5 of them can be found in the literature proposed by the other researchers and 71 of them are novel structures.
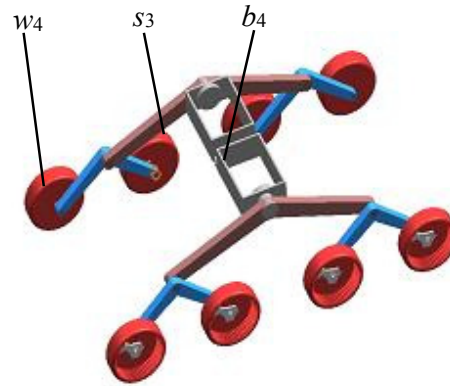
4.2 Non-isomorphic-combination synthesis and enumeration

Section 4.1 presents the synthesis of wheeled robots based on the isomorphic-combination mode and 76 types of structures for wheeled robot have been generated. In this section, we focus on the synthesis and enumeration of structures for the wheeled robots by using the non-isomorphic-combination synthesis mode. As discussed in Sect. 2, in the non-isomorphic-combination synthesis mode, for each structure to be synthesized, there must be at least two different types of wheel modules involved.

4.2.1 Synthesis of structures for four-wheeled robots

The synthesis of wheeled robot based on the non-isomorphic-combination synthesis mode starts from the synthesis of structures for four-wheeled robots. In this synthesis, the following component modules presented in Sect. 3 are considered: (a) the wheel module set $W = \{w_1, w_2, w_3, w_4\}$, (b) the suspension module subset $S = \{s_1\}$, and (c) the chassis module sets $B_1 = \{b_1, b_2, b_3\}$ and the segmented-chassis module subset $B_2 = \{b_4, b_5\}$. With these component modules, if considering the integrated-chassis only, according to Eq. (11), theoretically the degrees of choice for a four-wheeled robot generated through the non-isomorphic-combination synthe-
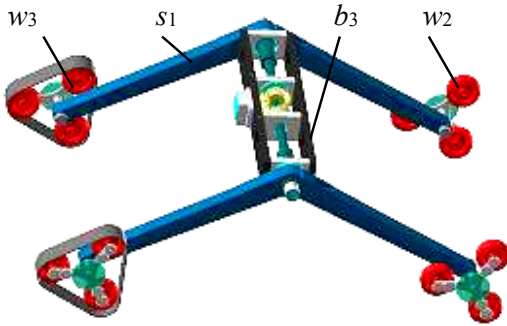
Figure 12. A type w_{23}-b_3-s_1 four-wheeled robot generated by non-isomorphic combination.

sis mode is

$$D_C''(R_{NI4-1}) = \left(C_4^2 + C_4^3 + C_4^4\right) \times M_1 \times N_1 = 11 \times 1 \times 3 = 33 \tag{18}$$

Where, $M_1 = D_C(S_1) = 1$ and $N_1 = D_C(B_1) = 3$.

However, in practical applications, in order to achieve better balance and locomotion performance, symmetric layout is adopted in the four-wheeled robot design such that the cases of integrating a wheel module subset W_i that contains three or four different types of wheel mechanisms/structures will not be considered. Therefore, in this section, in order to synthesize feasible four-wheeled robot, the maximum number of mechanisms/structures involved in one wheel module subset is $l_{1max} = D_C(W_i)_{1max} = 2$ such that the combinations of wheel modules in the cases C_4^3 and C_4^4 are not taken into account. Further, similar to the isomorphic-combination synthesis, structure of a wheeled robot with a rigid suspension s_1 can be reconfigured in both left-and-right layout and fore-and-aft layout. Hence, considering the above two additional points, by revising Eq. (18), the reasonable degrees of choice of structures for a four-wheeled robot that can be synthesized in this category is

$$D_C'(R_{NI4-1}) = 2 \times C_4^2 \times M_1 \times N_1 = 2 \times 6 \times 1 \times 3 = 36 \tag{19}$$

In these 36 structures, 18 of them are constructed with suspension in the right-and left layout and the other 18 types are generated with suspension in the fore-and-aft layout. All the 18 design schemes in the right-and-left layout are novel ones and they are listed in Table 8. In the table, w_{ab} denotes a wheel module subset W_i containing both wheel mechanisms/structures w_a and w_b with $a < b$ and $\{a, b\} \in \{1, 2, 3, 4\}$.

Figure 12 shows the structure of a type w_{23}-b_3-s_1 scheme four-wheeled robot, that is synthesized in this category. It contains two wheel modules, i.e. one exterior-planetary wheel module w_2 and one planetary-tracked wheel module w_3, a rigid suspension s_1 and a differential chassis b_3.

Furthermore, the 18 structures in the fore-and-aft layout are listed in Table 9. In the table, $\bar{s}$ denotes the suspen-

sion module that is configured in the fore-and-aft format. In these 18 design schemes, 6 of them, as shown in the first row of Table 9 with symbol "$+$" in the superscript, which are generated by combining the suspension module s_1, the rigid body b_1 and 2-combination of the wheel module set $W = \{w_1, w_2, w_3, w_4\}$ are functionally the same as those 6 schemes listed in the first row of Table 8 with the suspension in the left-and-right layout. Thus, there are 12 design schemes obtained in this category and they are all novel ones.

From Tables 8 and 9, it can be found that the actually degrees of choice of the structures for the four-wheeled space-exploring robot that adopts the integrated chassis module is

$$D_C(R_{NI4-1}) = D_C'(R_{NI4-1}) - 6 = 36 - 6 = 30 \tag{20}$$

and they are all new schemes.

In addition, considering those design schemes that adopt the segmented-body module subset $B_2 = \{b_4, b_5\}$, the additional degrees of choice of the structures for a four-wheeled mobile robot that are synthesized in this non-isomorphic-combination synthesis mode is

$$D_C(R_{NI4-2}) = C_4^2 \times M_1 \times N_2 = 6 \times 1 \times 2 = 12 \tag{21}$$

where $N_2 = D_C(B_2) = 2$.

Referring to Eq. (12) we get 12 more types of design schemes, they are all new structures and are listed in Table 10.

Therefore, including all the structures listed in Tables 8, 9 and 10, the total number of structures for the four-wheeled space-exploring robots synthesized using the non-isomorphic-combination mode is

$$N(R_{NI4}) = D_C(R_{NI4-1}) + D_C(R_{NI4-2}) = 30 + 12 = 42 \tag{22}$$

All these 42 types are new and feasible design schemes.

4.2.2 Synthesis of structures for six-wheeled robot

This section focuses on the synthesis of structures for six-wheeled robot based on non-isomorphic-combination synthesis mode. The component modules presented in Sect. 3 to be used are: (a) the wheel module set $W = \{w_1, w_2, w_3, w_4\}$, (b) the suspension module subset $S_2 = \{s_2, s_4, s_5\}$ and (c) the integrated chassis module subset $B_1 = \{b_1, b_2, b_3\}$. Since the purpose of this section is to synthesize feasible structures for six-wheeled robot, considering the requirement for symmetric layout so as to achieve better balance and locomotion performance, the maximum number of wheel mechanisms/structures can be used in one wheel module configuration is $l_{2max} = D_C(W_i)_{2max} = 3$, so the combination C_4^4 will not be considered. Thus, referring to Eq. (11), the degrees of choice of the structures for six-wheeled robots based on the

Table 8. Structures for four-wheeled robots $R_{\text{NI4}-1}$ in left-and-right layout.

	w_{12}	w_{13}	w_{14}	w_{23}	w_{24}	w_{34}
b_1	w_{12}-b_1-s_1	w_{13}-b_1-s_1	w_{14}-b_1-s_1	w_{23}-b_1-s_1	w_{24}-b_1-s_1	w_{34}-b_1-s_1
b_2	w_{12}-b_2-s_1	w_{13}-b_2-s_1	w_{14}-b_2-s_1	w_{23}-b_2-s_1	w_{24}-b_2-s_1	w_{34}-b_2-s_1
b_3	w_{12}-b_3-s_1	w_{13}-b_3-s_1	w_{14}-b_3-s_1	w_{23}-b_3-s_1	w_{24}-b_3-s_1	w_{34}-b_3-s_1

Table 9. Structures for four-wheeled robots $R_{\text{NI4}-1}$ in fore-and-aft layout.

	w_{12}	w_{13}	w_{14}	w_{23}	w_{24}	w_{34}
b_1	w_{12}-b_1-$\bar{s}_1^+$	w_{13}-b_1-$\bar{s}_1^+$	w_{14}-b_1-$\bar{s}_1^+$	w_{23}-b_1-$\bar{s}_1^+$	w_{24}-b_1-$\bar{s}_1^+$	w_{34}-b_1-$\bar{s}_1^+$
b_2	w_{12}-b_2-$\bar{s}_1$	w_{13}-b_2-$\bar{s}_1$	w_{14}-b_2-$\bar{s}_1$	w_{23}-b_2-$\bar{s}_1$	w_{24}-b_2-$\bar{s}_1$	w_{34}-b_2-$\bar{s}_1$
b_3	w_{12}-b_3-$\bar{s}_1$	w_{13}-b_3-$\bar{s}_1$	w_{14}-b_3-$\bar{s}_1$	w_{23}-b_3-$\bar{s}_1$	w_{24}-b_3-$\bar{s}_1$	w_{34}-b_3-$\bar{s}_1$

Figure 13. A type w_{34}-b_3-s_2 six-wheeled robot generated by non-isomorphic combination,
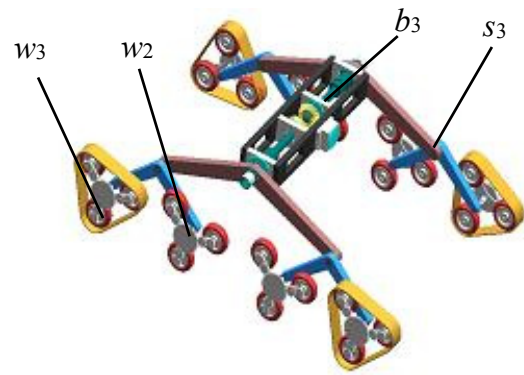
Figure 14. A type w_{23}-b_3-s_3 eight-wheeled robot generated by non-isomorphic combination.

non-isomorphic-combination synthesis mode is

$$D_{\text{C}}(R_{\text{NI6}}) = \sum_{l=2}^{l_{2\text{max}}} C_L^l \times D_{\text{C}}(S_2) \times D_{\text{C}}(B_1)$$
$$= \left(C_4^2 + C_4^3\right) \times 3 \times 3 = 90 \tag{23}$$

Therefore, according to the relation between Eqs. (11) and (12), there are totally $N(R_{\text{NI6}}) = D_{\text{C}}(R_{\text{NI6}}) = 90$ structures that can be obtained in this synthesis category and all these 90 structures are new design schemes. The results are listed in Table 11. In Table 11, w_{ab} denotes a member of a wheel module subset $W_i = \{w_a, w_b\}$ containing both wheel mechanisms/structures w_a and w_b with $a < b$ and $\{a, b\} \in \{1, 2, 3, 4\}$, and w_{abc} with $a < b < c$ and $\{a, b, c\} \in \{1, 2, 3, 4\}$ denotes an element of a wheel module subset $W_j = \{w_a, w_b, w_c\}$ that is composed of three wheel mechanisms/structures w_a, w_b and w_c.

An example of the structure for a six-wheeled space-exploring robot, i.e. type w_{34}-b_3-s_2 synthesized in the section is shown in Fig. 13. It is composed of four planetary-tracked wheels w_3, two interior-planetary wheels w_4, two rocker-boogie suspensions s_2 and a differential chassis b_3.

4.2.3 Structure synthesis of eight-wheeled robot

Similarly, by using the component modules provided in Sect. 3 including (a) the wheel module set $W = \{w_1, w_2, w_3, w_4\}$, (b) the suspension module subset $S_3 = \{s_3\}$ and (c) the integrated-chassis module subset $B_1 = \{b_1, b_2, b_3\}$, the structures for eight-wheeled robots can also be generated based on the non-isomorphic-combination synthesis mode. Figure 14 shows a structure of an eight-wheeled robot that is synthesized in this section. It is type w_{23}-b_3-s_3 scheme consisting of four exterior-planetary wheels w_2, four planetary-tracked wheels w_3, a rocker-bogie suspension s_3 and a differential chassis b_3.

Based on the rule for the non-isomorphic-combination synthesis mode and referring to Eq. (11), the degrees of choice for the structures of an eight-wheeled space-exploring robots synthesized in this category is

Table 10. Structures for four-wheeled robots R_{NI4-2}.

	w_{12}	w_{13}	w_{14}	w_{23}	w_{24}	w_{34}
b_4	w_{12}-b_4-s_1	w_{13}-b_4-s_1	w_{14}-b_4-s_1	w_{23}-b_4-s_1	w_{24}-b_4-s_1	w_{34}-b_4-s_1
b_5	w_{12}-b_5-s_1	w_{13}-b_5-s_1	w_{14}-b_5-s_1	w_{23}-b_5-s_1	w_{24}-b_5-s_1	w_{34}-b_5-s_1

Table 11. Structures for six-wheeled robots R_{NI6}.

	w_{12}	w_{13}	w_{14}	w_{23}	w_{24}
b_1	w_{12}-b_1-s_2 w_{12}-b_1-s_4 w_{12}-b_1-s_5	w_{13}-b_1-s_2 w_{13}-b_1-s_4 w_{13}-b_1-s_5	w_{14}-b_1-s_2 w_{14}-b_1-s_4 w_{14}-b_1-s_5	w_{23}-b_1-s_2 w_{23}-b_1-s_4 w_{23}-b_1-s_5	w_{24}-b_1-s_2 w_{24}-b_1-s_4 w_{24}-b_1-s_5
b_2	w_{12}-b_2-s_2 w_{12}-b_2-s_4 w_{12}-b_2-s_5	w_{13}-b_2-s_2 w_{13}-b_2-s_4 w_{13}-b_2-s_5	w_{14}-b_2-s_2 w_{14}-b_2-s_4 w_{14}-b_2-s_5	w_{23}-b_2-s_2 w_{23}-b_2-s_4 w_{23}-b_2-s_5	w_{24}-b_2-s_2 w_{24}-b_2-s_4 w_{24}-b_2-s_5
b_3	w_{12}-b_3-s_2 w_{12}-b_3-s_4 w_{12}-b_3-s_5	w_{13}-b_3-s_2 w_{13}-b_3-s_4 w_{13}-b_3-s_5	w_{14}-b_3-s_2 w_{14}-b_3-s_4 w_{14}-b_3-s_5	w_{23}-b_3-s_2 w_{23}-b_3-s_4 w_{23}-b_3-s_5	w_{24}-b_3-s_2 w_{24}-b_3-s_4 w_{24}-b_3-s_5
	w_{34}	w_{123}	w_{124}	w_{134}	w_{234}
b_1	w_{34}-b_1-s_2 w_{34}-b_1-s_4 w_{34}-b_1-s_5	w_{123}-b_1-s_2 w_{123}-b_1-s_4 w_{123}-b_1-s_5	w_{124}-b_1-s_2 w_{124}-b_1-s_4 w_{124}-b_1-s_5	w_{134}-b_1-s_2 w_{134}-b_1-s_4 w_{134}-b_1-s_5	w_{234}-b_1-s_2 w_{234}-b_1-s_4 w_{234}-b_1-s_5
b_2	w_{34}-b_2-s_2 w_{34}-b_2-s_4 w_{34}-b_2-s_5	w_{123}-b_2-s_2 w_{123}-b_2-s_4 w_{123}-b_2-s_5	w_{124}-b_2-s_2 w_{124}-b_2-s_4 w_{124}-b_2-s_5	w_{134}-b_2-s_2 w_{134}-b_2-s_4 w_{134}-b_2-s_5	w_{234}-b_2-s_2 w_{234}-b_2-s_4 w_{234}-b_2-s_5
b_3	w_{34}-b_3-s_2 w_{34}-b_3-s_4 w_{34}-b_3-s_5	w_{123}-b_3-s_2 w_{123}-b_3-s_4 w_{123}-b_3-s_5	w_{124}-b_3-s_2 w_{124}-b_3-s_4 w_{124}-b_3-s_5	w_{134}-b_3-s_2 w_{134}-b_3-s_4 w_{134}-b_3-s_5	w_{234}-b_3-s_2 w_{234}-b_3-s_4 w_{234}-b_3-s_5

$$
D_C(R_{NI8}) = \sum_{l=2}^{L} C_L^l \times M_3 \times N_1
$$
$$
= \left(C_4^2 + C_4^3 + C_4^4\right) \times 1 \times 3 = 33 \qquad (24)
$$

Where, $L = D_C(W) = 4$, $M_3 = D_C(S_3) = 1$ and $N_1 = 3$ is the same as that in Eq. (18).

Therefore, according the Eq. (12), there are $N(R_{NI8}) = D_C(R_{NI8}) = 33$ structures attained in this section for generating eight-wheeled robots and they are all new design schemes; the results are listed in Table 12.

Hence, summarizing all the structures obtained from Tables 8 to 12, the total number of structures for wheeled robots that are synthesized based on the non-isomorphic-combination synthesis mode can be calculated as

$$
N(R_{NI}) = D_C(R_{NI}) = N(R_{NI4}) + N(R_{NI6}) + N(R_{NI8})
$$
$$
= 42 + 90 + 33 = 165 \qquad (25)
$$

This also implies that there are 165 non-isomorphic structure schemes to be chosen for designing a feasible desired wheeled robot based on the specific functions required. All these 165 schemes are new ones.

As a result, using structure synthesis for wheeled robots with isomorphic and non-isomorphic module combinations, the number of structures for wheeled robot achieved in this paper is

$$
N(R) = N(R_I) + N(R_{NI}) = 76 + 165 = 241 \qquad (26)
$$

In these 241 design schemes, only 5 of them are existing structures that can be found in literature (as listed in Table 13), and the remaining 236 types are all novel which provide a wide range of choices for wheeled mobile robot design. Furthermore, since all the structures are synthesized by integrating of three elemental modules, one type of the robot structure can be conveniently reconfigured to the other type by simply changing the appropriate modules according to the functions desired by specific applications. The properties and performance of the proposed structures for wheeled robots are evaluated in the following section and consequently physcial prototypes of some types of the proposed wheeled robots are built and tested.

Table 12. Structures for eight-wheeled robots R_{NI8}.

	w_{12}	w_{13}	w_{14}	w_{23}	w_{24}	w_{34}
b_1	w_{12}-b_1-s_3	w_{13}-b_1-s_3	w_{14}-b_1-s_3	w_{23}-b_1-s_3	w_{24}-b_1-s_3	w_{34}-b_1-s_3
b_2	w_{12}-b_2-s_3	w_{13}-b_2-s_3	w_{14}-b_2-s_3	w_{23}-b_2-s_3	w_{24}-b_2-s_3	w_{34}-b_2-s_3
b_3	w_{12}-b_3-s_3	w_{13}-b_3-s_3	w_{14}-b_3-s_3	w_{23}-b_3-s_3	w_{24}-b_3-s_3	w_{34}-b_3-s_3
	w_{123}	w_{124}	w_{134}	w_{234}	w_{1234}	–
b_1	w_{123}-b_1-s_3	w_{124}-b_1-s_3	w_{134}-b_1-s_3	w_{234}-b_1-s_3	w_{1234}-b_1-s_3	–
b_2	w_{123}-b_2-s_3	w_{124}-b_2-s_3	w_{134}-b_2-s_3	w_{234}-b_2-s_3	w_{1234}-b_2-s_3	–
b_3	w_{123}-b_3-s_3	w_{124}-b_3-s_3	w_{134}-b_3-s_3	w_{234}-b_3-s_3	w_{1234}-b_3-s_3	–

Table 13. Existing structures.

| Existing robot	w_1-b_1-s_1	w_2-b_1-s_1	w_1-b_5-s_1	w_1-b_3-s_2	w_1-b_3-s_3
Sources	Apollo 15	Lunar rover, see Gao et al. (2005)	Widely used in segmented vehicle	Sojourner Curiosity YUTU	Lunar robot, see Eom et al. (2014)

5 Simulation and prototype evaluation

In this section, feasibility of the structures for wheeled robots proposed in Sect. 4 are evaluated based on virtual prototypes, mathematical models and physical prototype to provide information for product development and the subsequent experimental studies.

5.1 Simulation based on virtual prototype

The virtual prototype technology provides an efficient and intuitive tool that can be used to build up the entire product model digitally, and subsequently to simulate and analyse the performance of the proposed product virtually in different kinds of working conditions. It helps to assess performance of the product and provide suggestions for optimising the design and hence improving the produce functions.

In this paper, a software platform is developed by integrating the ADAMS® software with the control package provided by Matlab®/Simulink® for constructing virtual models of the structures of wheeled robots synthesized in Sect. 4 and also simulating and evaluating their functions and performance. The platform we developed has the functions of supporting module definition, processing module combination, implementing performance evaluation and conducting design optimization. The flow chart diagram of the procedures of the software platform is shown in Fig. 15.

In order to simulate and evaluate a specified design of a wheeled robot, by following the procedures illustrated in Fig. 15, we firstly build the dynamic and control models of all component modules based on the dynamics package in the ADMAS system and the control package in the Matlab/Simulink system, respectively. Then we combine component modules into the integrated virtual robot proto-
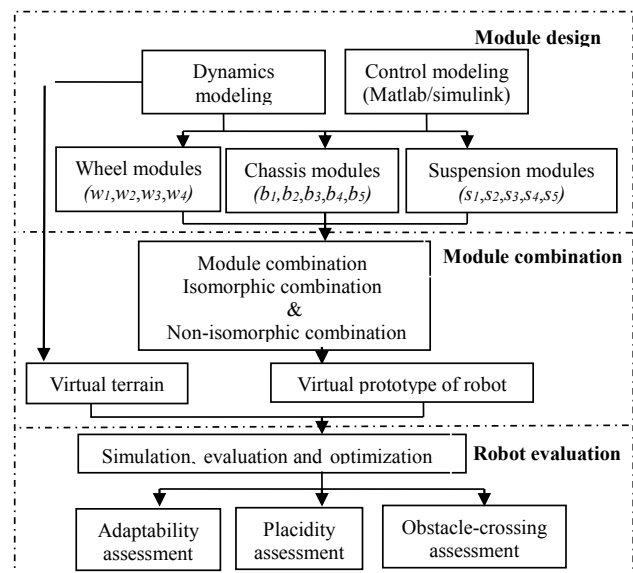
Figure 15. Procedures for virtual simulation and evaluation of space rover.

type. Thereafter, a predefined virtual terrain environment is used to test the mobility of the robot, including capacity of geometric-passing, obstacle-crossing, anti-capsizal, smooth-ride, etc. Finally, we can optimize the parameters of the robot and make decision on the choice of design schemes.

An instance robot is designed in this section to demonstrate the simulation and evaluation by using the proposed software platform. This is a six-wheeled robot, i.e. w_4-b_3-s_4 synthesized based on the isomorphic-combination mode consisting of six wheel modules w_4, one chassis module b_3 and two suspension modules s_4. In the detailed design, radius of

the wheel is 80 mm, the distance between the two adjacent wheels is 300 mm, and the width of the robot is 450 mm. In the virtual prototype, material properties for each component were properly assigned and information for terrain environment was defined.

In the simulation, the robot can climb a slope of 35°, as shown in Fig. 16a, and can cross over various typical blocks and craters with heights of 60 mm facilely, as shown in Fig. 16b. In the evaluation of driving smoothness, the gravity height of the front wheel, middle wheel, rear wheel are 60 mm (see Fig. 16d) when the robot climbs a 60 mm height obstacle, while the gravity height change of chassis is nearly 35 mm (see Fig. 16d), which is much smaller than that of the six wheels, this validate that the robot has excellent driving smoothness. Fig. 16e shows the contact forces of the six wheels, Fig. 16f shows the contact force of the front wheel, by comparing Fig. 16e with Fig. 16f, we found that the contact forces of the six wheels are relatively homogeneous, this validates the force smoothness performance of the proposed robot.

5.2 Mathematical models for traverse performance evaluation

The vehicle traversing theory shows that the traverse ability and versatility of a vehicle are enhanced with the increase of wheel number. However, once the number of wheels is determined, the design of the suspension system associated with the wheel system becomes important and the feature of the whole mechanical system needs to be evaluated. Thus, in order to provide better solutions for practical space-exploring rover design, the following desired features are considered in the structure evaluation:

1. Ground adaptability. As a space rover, its wheels must have excellent adaptability to follow the contours of different kinds of terrains. The contact forces between the wheels and the terrain are expected to be smooth, so as to obtain the maximal ground adhesion forces and prevent single wheel from getting stuck in the ground. In order to get the maximal ground adhesion forces, self-adaptability model of a single wheel can be formulated as

$$V_s(t) = \frac{F_c(t) - F_f}{F_f} \qquad (27)$$

Where, $F_c(t)$ is the wheel-ground contact force at time t, F_f is the wheel-ground contact force on a flat terrain, and $V_s(t)$ is the coefficient of self-adaptability of the wheel at time t.

2. Driving smoothness. Considering autonomous navigation and instrument safety, a space rover should drive placidly. Driving smoothness is mainly assessed based on the varying range and frequency of the pitch angle, the roll angle and the height of the rover chassis centre. The varying range is determined by the suspension structure; while the varying frequency is influenced by the control characteristic of autonomous navigation. Especially, the variation of the height of the rover chassis centre has a significant effect on driving smoothness. The average values of the height of body centre $h(t)$, the pitch angle $\alpha(t)$ and the roll angle $\beta(t)$, can be used for evaluating driving smoothness of the space-exploring wheeled robots. The disperse degree of $h(t)$ can be evaluated by its mean square, which is expressed as

$$\sigma_h^2(t) = E\{[h(t) - \overline{h}]^2\} \qquad (28)$$

where, $\sigma_h^2(t)$ denotes the mean square of $h(t)$, E denotes the arithmetic of average value, and $\overline{h}$ is the average value of $h(t)$. The same function can be used for measuring the pitch angle α and roll angle β, which can be expressed as $\sigma_\alpha^2(t)$ and $\sigma_\beta^2(t)$, respectively.

3. Obstacle-crossing capability. It is determined by the suspension system and the wheels. The suspension system distributes the load of weight equally to all the wheels. If the suspension systems are similar, the diameter, the width and the spiral fin of the wheel become decisive factors. If the parameters of mass and power are determined, the margin of obstacle-crossing capability can be reflected by the height of the obstacle h' that the rover can cross over, The larger height h' is, the better obstacle-crossing capability of the robot has.

5.3 Physical prototype development and tests

Based on the simulation and evaluation results obtained in the software platform, optimal and detailed designs of several types of wheeled robots were conducted and physical prototypes of the modules and robots were fabricated, assembled and integrated with low-level control system, vision system and sensors.

Figure 17 shows the physical prototypes of three different types of wheeled robots: a four-wheeled robot (w_3-b_3-s_1), as shown in Fig. 17a, consisting of four planetary-tracked wheels w_3, a differential chassis b_3, and two rigid suspensions s_1; a novel six-wheeled robot, i.e. w_4-b_3-s_2 as illustrated in Fig. 17b, containing six interior-planetary wheels w_4, a differential chassis b_3, and two rocker-boogie suspensions s_2; and another new six-wheeled robot (w_1-b_3-s_5) that is composed of six integration wheels w_1, a differential chassis b_3 and two four-bar linkage integrated suspensions s_5. The virtual simulation, evaluation and field tests indicated
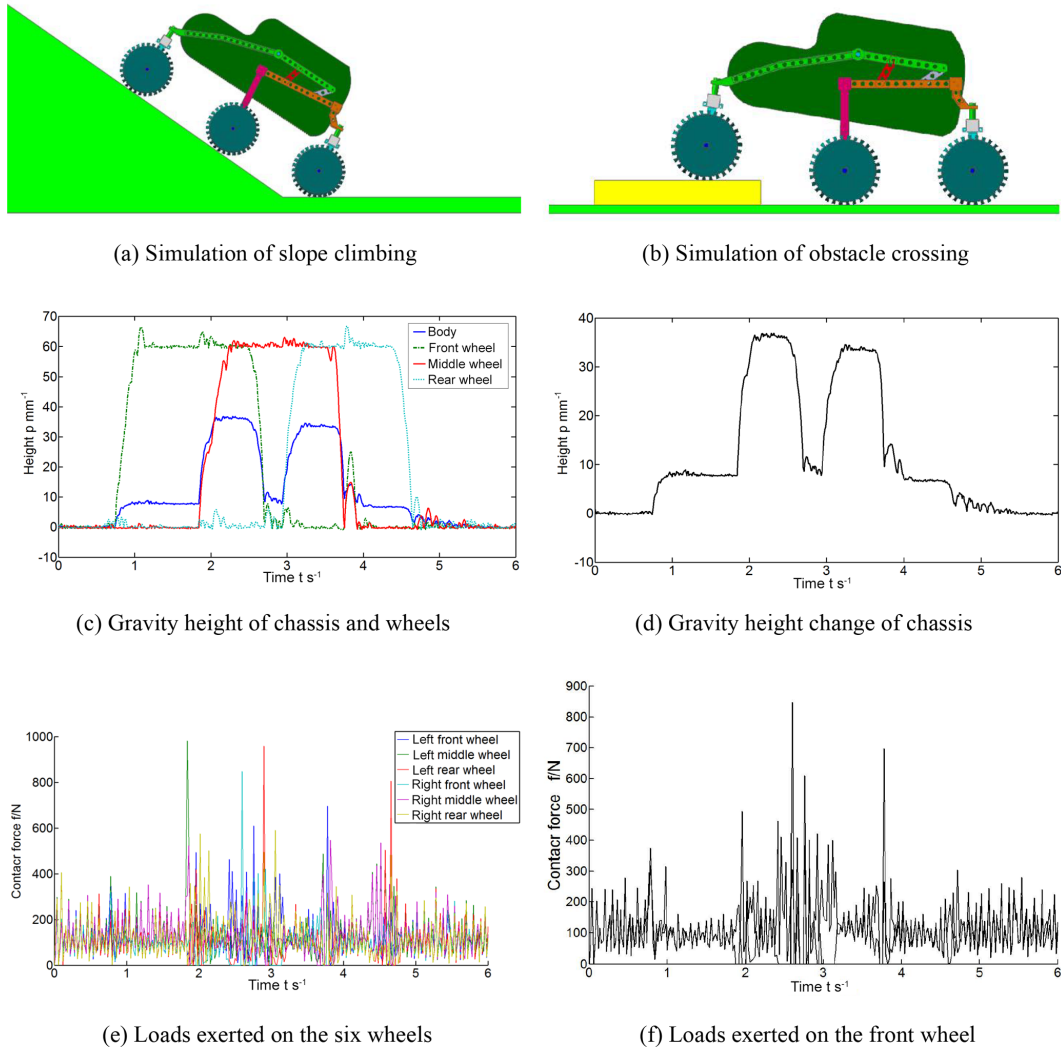
(a) Simulation of slope climbing

(b) Simulation of obstacle crossing

(c) Gravity height of chassis and wheels

(d) Gravity height change of chassis

(e) Loads exerted on the six wheels

(f) Loads exerted on the front wheel

Figure 16. Simulation and evaluation of a six-wheeled rover in virtual environment.

(a) Four-wheeled w_3-b_3-s_1

(b) Six-wheeled w_4-b_3-s_2

(c) Six-wheeled w_1-b_3-s_5
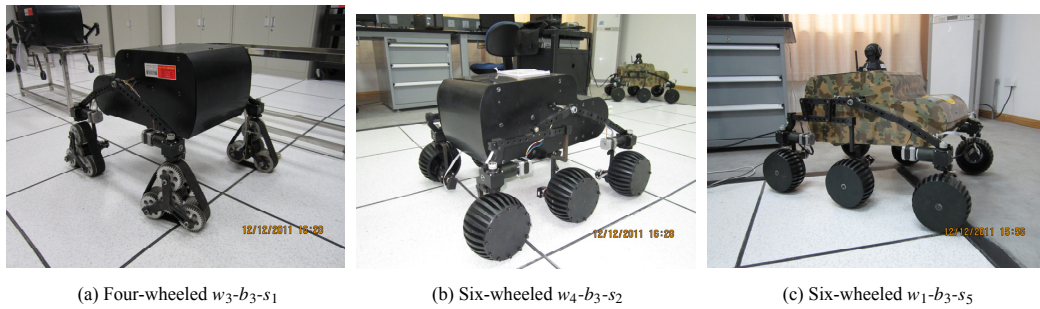
Figure 17. Prototypes of three types of wheeled robots.

that all these three robots have excellent ground adaptability, driving smoothness and obstacle crossing capability. Taking the six wheeled robot (w_1-b_3-s_5) as an example, as shown in Fig. 18, this new robot has better smoothness compared with

classic rokie-bogie suspension robot (w_1-b_3-s_2) when both conquer the same obstacle with the height of 60 mm.

A series of systematic field tests were carried out on the physical prototype of the type w_1-b_3-s_5 six-wheeled robot so as to check the practical performances of all kinds of creative
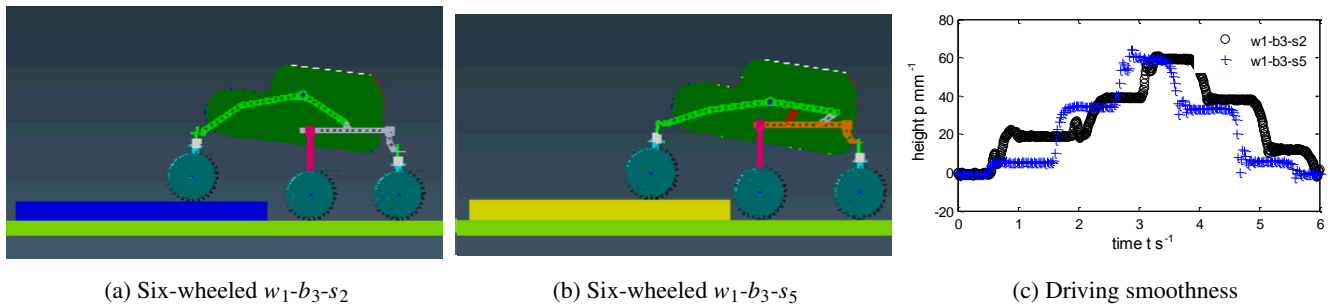
(a) Six-wheeled w_1-b_3-s_2 (b) Six-wheeled w_1-b_3-s_5 (c) Driving smoothness

Figure 18. Performance evaluation of type w_1-b_3-s_5 six-wheeled robot.

(a) Slope climbing   (b) Running on ground   (c) Turning around

(d) Front wheel crossing obstacle   (e) Middle wheel crossing obstacle   (f) Rear wheel crossing obstacle
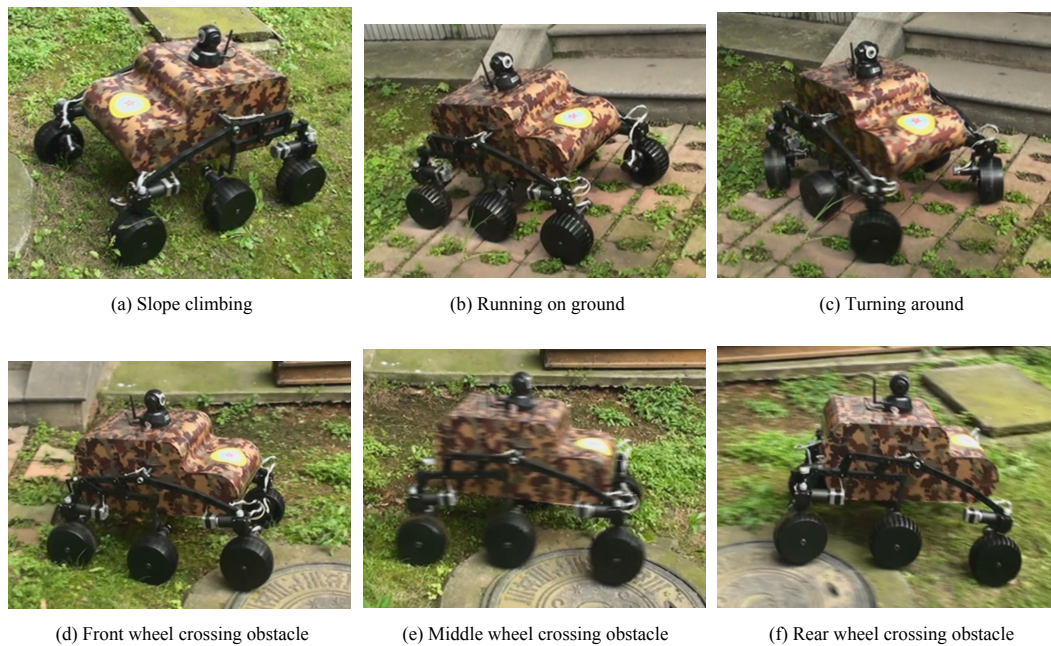
Figure 19. Performance of type w_1-b_3-s_5 six-wheeled robot.

robot locomotions. Some representative photos taken during the tests are illustrated in Fig. 19.

6 Conclusions

In this paper, a new approach was for the first time proposed for the structure synthesis of wheeled mobile robots. By defining fundamental component modules and adopting the concept of isomorphic and non-isomorphic, the proposed synthesis method was established and formulated using set theory and its associated operations. Referring to the classical component modules and through the innovative design, three elemental module sets were identified and characterised which include the wheeled module set formed by four types of wheel mechanisms; the suspension module set comprised of five types of mechanisms/structures; and the chassis module set constructed by five types of rigid or ar-

ticulated structures. All the component modules were then employed for the systematical synthesis of structures for four-, six-, and eight-wheeled robots in two synthesis categories, namely the isomorphic-combination synthesis mode and the non-isomorphic-combination synthesis mode, resulting in the generation of a family of structures of wheeled robots which contains as many as 241 members with 236 of them being new structures that were revealed for the first time. Furthermore, mathematical models and a software platform were developed so as to simulate and evaluate the terrain adaptability, driving smoothness and obstacle-crossing capability of the wheeled robots constructed based on the method proposed in this paper. Physical prototypes of selected wheeled rovers were subsequently designed, fabricated, assembled and integrated with low-level control system; leading to the initial experimental field tests for demonstrating and verifying the proposed novel robot structures.

The synthesis approach presented in this paper can be used for the synthesis of other module-based robotic systems and the 241 structures obtained in this paper provide a wide range of choices for constructing appropriate wheeled robots, i.e. rovers that can be used for space explorations of diverse missions. In addition, since all the structures synthesized in this paper were achieved by a combination of the three elemental modules, one type of the robot structure can be conveniently reconfigured to the other type by simply changing the appropriate modules according to the functions desired by specified applications. Hence, an efficient approach has been presented in this paper for the structure synthesis of wheeled mobile robot, and a human-in-loop software platform has been developed to evaluated these structures. In order to reduce workload for finding and synthesizing useful design, and to improve design efficiency and quality; the future work to be done will be implementing the automatic design of wheeled robot based on artificial intelligence technology.

Data availability. No data sets were used in this article.

References

Aoki, T., Murayama, Y., and Hirose, S.: Development of a Transformable Three-wheeled LunarRover: Tri-Star IV, J. Field Robot., 31, 206–223, 2014.

Arvidson, R. E. and Maimone, M.: Curiosity Rover Mobility Issues Crossing Martian Megaripple Fields, in: 47th Lunar and Planetary Science Conference, 249–254, LPI, The Woodlands, Texas, 2016.

Bares, J. E. and Wettergreen, D. S.: Lessons from the Development and Deployment of Dante II, Springer, London, 1998.

Bartlett, P. W., Wettergreen, D., and Whittaker, W.: Design of the Scarab Rover for Mobility & Drilling in the Lunar Cold Traps, in: Proceedings of the 9th International Symposium on Artificial Intelligence, Robotics and Automation in Space, 26–29 February 2008, Hollywood, USA, 2008.

Carrier, D.: Soviet rover systems, in: Proceedings of the AIAA Space Programs and Technologies Conference, 24–27, Huntsville, AL, 1992.

Chen, C., Wang, R., Yang, J., Guo, L., and Yang, L.: Design of a high performance suspension for lunar rover based on evolution, Acta Astronaut., 64, 925–934, 2009.

Ding, L., Deng, Z., Gao, H., Guo, J., Zhang, D., and Iagnemma, K. D.: Experimental study and analysis of the wheels'steering mechanics for planetary exploration wheeled mobile robots moving on deformable terrain, Int. J. Robot. Res., 32, 712–743, 2013.

Eom, W., Lee, J., Gong, H., and Choi, G.: Study on an 8-Wheel Suspension to Enhance the Hill-Climbing Performance for a Planetary Exploration Rover, J. Astron. Space Sci., 31, 347–351, 2014.

Fuke, Y. and Krotkov, E.: Dead Reckoning for a Lunar Rover om Uneven Terrain, in: Proceedings of the 1996 IEEE International Conference on Robotics and Automation, 411–416, 1996.

Gao, H., Deng, Z., Hu, M., and Wang, S.: Key Technology of Moving system of Lunar Rover With Planetary Wheel, Chin. J. Mech. Eng., 41, 156–161, 2005.

Ghotbi, B., Gonzlez, F., Kovecses, J., and Angeles, J.: A novel concept for analysis and performance evaluation of wheeled rovers, Mech. Mach. Theory, 83, 137–151, 2015.

Haggart, S. and Waydo, J.: The Mobility System Wheel Design for NASA's Mars Sinence Laboratory Mission, in: 11th European Conference of the International Society for Terrain-Vehicle Systems, Torino, Italy, 2008.

Huntsberger, T., Aghazarian, H., Backes, P., Baumgartner, E., Yang, C., Garrett, M., Kennedy, B., Leger, C., Magnone, L., Norris, J., Powell, M., Trebi-Ollennu, A., and Schenker, P.: FIDO rover field trials as rehearsal for the NASA 2003 Mars Exploration Rovers mission, in: 2002 Proceedings of the 5th Biannual World Automation Congress, 9–13 June, Orlando, FL, USA, 320–327, 2002.

Inotsume, H., Sutoh, M., Nagaoka, K., Nagatani, K., and Yoshida, K.: Modeling, Analysis, and Control of an Actively Reconfigurable Planetary Rover for Traversing Slopes Covered with Loose Soil, J. Field Robot., 30, 875–896, 2013.

Ip, W.-H., Yan, J., Li, C.-L., and Ouyang, Z.-Y.: Preface: The Chang'e-3 lander and rover mission to the Moon, Res. Astron. Astrophys., 14, 1511–1513, 2014.

Jain, A., Balaram, A. J., Cameron, J., Guineau, J., Lim, C., Pornerantz, M., and Sohl, G.: Recent Developments in the ROAMS Planetary Rover Simulation Environment, in: 2004 IEEE Aerospace Conference Proceedings, 6–13 March 2004, Big Sky, MT, USA, 861–876, 2004.

Kemurdjian, A., Gromov, V., Mishkinyuk, V., Kucherenko, V., and Sologub, P.: Small Marsokhod configuration, in: International Conference on Robotics and Automation, 1, 165–168, IEEE, Nice, France, 1992.

Kennedy, B., Agazarian, H., Cheng, Y., Garrett, M., Hickey, G., Huntsberger, T., Magnone, L., Mahoney, C., Meyer, A., and Knight, J.: LEMUR: Legged Excursion Mechanical Utility Rover, Autonomous Robots, 11, 201–205, 2001.

Krotkov, E., Bares, J., Katragadda, L., Simmons, R., and Whittaker, R.: Lunar rover technology demonstrations with Dante and Ratler, in: JPL, Third International Symposium on Artificial Intelligence, Robotics, and Automation for Space, 18–20 October 1994, Pasadena, California, USA, 113–116, 1994.

Lionel, E. E., Jason, D. D., Thomas, R. G., Scott, M. F., and Andre, P. M.: Performance Analysis and Technical Feasibility Assessment of a Transforming Roving-Rolling Explorer Rover for Mars Exploration, J. Mech. Design, 136, 1–11, 2014.

Luo, Z., Shang, J., and Zhang, Z.: Innovative design of six wheeled space exploration robot using module combination, in: Mechatronics and Machine Vision in Practice, 460–465, 2013.

Michaud, S., Richter, L., Thueer, T., Gibbesch, A., Huelsing, T., Schmitz, N., Weiss, S., Krebs, A., Patel, N., Joudrier, L., Siegwart, R., Schafer, B., and Ellery, A.: Rover Chassis Evaluation and Design Optimization Using the RCET, in: Proceedings of the 9th ESA Workshop on ASTRA, Noordwijk, the Netherlands, 2006.

Michaud, S., Gibbesch, A., Thueer, T., Krebs, A., Lee, C., Despont, B., Schfer, B., and Slade, R.: Development of the ExoMars Chassis and Locomotion Subsystem, in: I-Sairas 2008 – International Symposium on Artificial Intelligence, Robotics and Automation in Space, 26–29 February, Hollywood, USA, 849–876, 2008.

Putz, P.: Space robotics in Europe: A survey, Robot. Auton. Syst., 23, 3–16, 1998.

Richard, A. C.: The Mars exploration rover project, Acta Astronaut., 57, 116–120, 2005.

Rollins, E., Luntz, J., Foessel, A., and Shamah, B. E. A.: Nomad: a demonstration of the transforming chassis, in: Proceedings of the IEEE International Conference on Robotics and Automation, 1, 611–617, IEEE Robotics and Automation Society, IEEE, Leuven, 1998.

Schenker, P. S., Huntsberger, T. L., Pirjanian, P., Baumgartner, E. T., and Tunstel, E.: Planetary Rover Developments Supporting Mars Exploration,Sample Return and Future Human-Robotic Colonization, Autonomous Robots, 14, 103–126, 2003.

Seeni, A., Schafer, B., and Hirzinger, G.: Aerospace Technologies Advancements:Robot Mobility System for Planetary Surface Exploration – State-of-the-Art and Future, InTech, Croatia, USA, 2010.

Shang, J. Z., Luo, Z. R., and Li, S. Y.: Mobiltiy evaluation and innovation of wheeled space rover, Chin. J. Mech. Eng., 19, 187–190, 2006a.

Shang, J. Z., Luo, Z. R., and Zhang, X. F.: Two kinds of wheeled lunar rover suspension shecme and their virtual prototype simulation, China Mechanical Engineering, 17, 49–52, 2006b.

Siegwart, R., Lamon, P., Estier, T., Lauria, M., and Piguet, R.: Innovative design for wheeled locomotion in rough terrain, Robot. Auton. Syst., 40, 151–162, 2002.

Takshi, K., Kuroda, Y., Yasuharu, K., and Ichiro, N.: Small Lightweight Rover "Micro5" for Lunar Exploration, Acta Astronaut., 52, 447–453, 2003.

Tao, J., Deng, Z., Fang, H., Gao, H., and Yu, X.: Development of a Wheeled Robotic Rover in Rough Terrains, in: Proceedings of the 6th World Congress on Intelligent Control and Automation, 21–23 June 2006, Dalian, China, 2006.

Thueer, T. and Siegwart, R.: Mobility evaluation of wheeled all-terrain robots, Robot. Auton. Syst., 58, 508–519, 2010.

Tsai, L.-W.: Mechanism design: enumeration of kinematic structures according to function, CRC Press, Florida, USA, 2000.

Tunstel, E.: Evolution of Autonomous Self-Righting Behaviors for Articulated Nanorovers, in: Artificial Intelligence, Robotics and Automation in Space, Proceedings of the Fifth International Symposium, ISAIRAS '99, edited by: Perry, M., 341–346, Paris: European Space Agency, ESTEC, Noordwijk, the Netherlands, 1999.

Tunstel, E., Huntsberger, T., Aghazarian, H., Backes, P., Baumgartner, E., Cheng, Y., Garrett, M., Kennedy, B., Leger, C., Magnone, L., Norris, J., Powell, M., Trebi-Ollennu, A., and Schenker, P.: FIDO rover field trials as rehearsal for the NASA 2003 mars exploration rovers mission, in: Automation Congress, 2002 Proceedings of the 5th Biannual World, 14, 320–327, IEEE, 2002.

Volpe, R., Balaram, J., Ohm, T., and Ivlev, R.: Rocky 7: A next generation mars rover prototype, J. Adv. Robot., 11, 341–358, 1997.

Wen, G., Ma, C., Cheng, D., Q.T., J., Chen, Z., Yang, X., Yin, H., and Zhou, J.: A Four-Wheel-Rhombus-Arranged Mobility System for a New Lunar Robotic Rover, Int. J. Adv. Robot. Syst., 10, 1–10, 2013.

Wilson, J.: How we'll get back to the moon, GoddardView, 1, 2–3, 2005.

Winnendael, M. V. and Visentin, G.: Nanokhod microrover heading towards Mars, in: Proceedings of the Fifth International Symposium on ArtificialIntelligence, Robotics and Automation in Space, 69–76, Natioanal Aeronautics and Space Adminstration, Jet Propulsion Laboratory, Pasadena, California, 1999.

Yang, Y. C., Bao, J. S., Jin, Y., and Cheng, Y. L.: A Virtual Simulation Environment for Lunar Rover: Framework and Key Technologies, International J. Adv. Robot. Syst., 5, 201–208, 2008.

Yen, J., Jain, A., and Balaram, J.: ROAMS: Rover Analysis Modeling and Simulation, in: Proceedings of the Fifth International Symposium on Artifiial Intelligence, Robotics and Automation in Space, 249–254, Paris: European Space Agency, Noordwijk, the Netherlands, 1999.